Published as J. Chem. Phys. **142**, 084118 (2015), http://dx.doi.org/10.1063/1.4913291.
This is a corrected version of the accepted manuscript.

Towards Time-Dependent Current-Density-Functional Theory in the non-linear regime

J. M. Escartín,[1,2,3] M. Vincendon,[1,2] P. Romaniello,[4] P. M. Dinh,[1,2] P.-G. Reinhard,[5] and E. Suraud[1,2]
[1)] *Université de Toulouse, UPS, Laboratoire de Physique Théorique, IRSAMC, F-31062 Toulouse Cedex, France*
[2)] *CNRS, UMR5152, F-31062 Toulouse Cedex, France*
[3)] *Theory of Condensed Matter Group, Cavendish Laboratory, University of Cambridge, J.J. Thomson Avenue, Cambridge CB3 0HE, United Kingdom*
[4)] *Laboratoire de Physique Théorique, CNRS, IRSAMC, Université Toulouse III - Paul Sabatier and European Theoretical Spectroscopy Facility, 118 Route de Narbonne, 31062 Toulouse Cedex, France*
[5)] *Institut für Theoretische Physik, Universität Erlangen, Staudtstraße 7, D-91058 Erlangen, Germany*

Time-Dependent Density-Functional Theory (TDDFT) is a well-established theoretical approach to describe and understand irradiation processes in clusters and molecules. However, within the so-called adiabatic local density approximation (ALDA) to the exchange-correlation (xc) potential, TDDFT can show insufficiencies, particularly in violently dynamical processes. This is because within ALDA the xc potential is instantaneous and is a local functional of the density, which means that this approximation neglects memory effects and long-range effects. A way to go beyond ALDA is to use Time-Dependent Current-Density-Functional Theory (TDCDFT), in which the basic quantity is the current density rather than the density as in TDDFT. This has been shown to offer an adequate account of dissipation in the linear domain when the Vignale-Kohn (VK) functional is used. Here, we go beyond the linear regime and we explore this formulation in the time domain. In this case, the equations become very involved making the computation out of reach; we hence propose an approximation to the VK functional which allows us to calculate the dynamics in real time and at the same time to keep most of the physics described by the VK functional. We apply this formulation to the calculation of the time-dependent dipole moment of Ca, Mg and Na_2. Our results show trends similar to what was previously observed in model systems or within linear response. In the non-linear domain, our results show that relaxation times do not decrease with increasing deposited excitation energy, which sets some limitations to the practical use of TDCDFT in such a domain of excitations.

I. INTRODUCTION

Reactions with photons serve since the event of quantum physics as a crucial tool for the analysis of atoms and molecules, a tool which has been refined in the course of time, experimentally as well as theoretically.[1] Photoreactions have become extremely popular with the advent of coherent light sources whose enormous progresses allow meanwhile to trigger and to track photon-induced electron dynamics in a time-resolved manner.[2] This calls, at the theoretical side, for reliable and detailed modelling. Among the various available approaches, Time-Dependent Density Functional Theory (TDDFT) offers an optimal compromise. Within this approach, one needs to approximate the so-called exchange-correlation potential which contains the many-body effects (beyond Hartree) of the system. The standard approximation is the Adiabatic Local Density Approximation (ALDA), in which the ground-state local density approximation is evaluated at the instantaneous local density. Although ALDA provides a sound starting basis for describing dynamical processes, it is still plagued by intrinsic limitations. One of them concerns the account of dissipative effects which require to go beyond ALDA. The main characteristic of the ALDA is that it is local in time as well as in space. Vignale and Kohn showed for the case of time-dependent linear response theory that a frequency-dependent local-density approximation of the exchange-correlation potential does not exist in general, but that a local approximation can be maintained if the theory is extended to also include the current density.[3,4] Therefore, it can be more convenient and more efficient to use a local functional of the current density rather than a non-local functional of the density. By studying a weakly perturbed electron gas, Vignale and Kohn derived an exchange-correlation vector potential that is a local functional of the current density.[4] This functional has been used since then for the description of finite and infinite electronic systems within the linear-response regime. One of the successes of this approach is that the use of the local current-density functional puts the polarizability of conjugated polymers into the right order of magnitude, while it was grossly overestimated in ALDA.[5,6] In extended systems, it is able to describe the electron-electron scattering responsible for the Drude-like tail in metals, a feature which is completely absent within ALDA.[7] TDCDFT can also be used beyond linear response in a real-time description. Such an extension has already been studied, but so far for models or simple systems[8–10] in which, thanks to the considered space symmetries, the complexity of the equations reduces to that of TDDFT. These studies indicate that the VK introduce an artificial damping of electron dynamic, which was also observed in the linear response of atoms.[11] It becomes then important to further explore the VK functional. It is the aim of this work to investigate TDCDFT with the VK functional in the real-time domain for realistic systems in full three space dimensions. The outline of this article is as follows. In Sec. II, we summarize the key equations of TDCDFT, we introduce the VK functional, and we

show how one can approximate it to make calculations feasible. We report the main aspects of the implementation in Sec. III. In Sec. IV, we present results for the time evolution of the dipole moment of Ca, Mg, and Na_2, we compare the excitation energies with previous works using VK in the linear regime, and we explore the nonlinear regime. Finally, we give our conclusions in Sec. V.

II. THEORY

Standard TDDFT employs a scalar multiplicative Kohn-Sham potential $V_\mathrm{S}(\mathbf{r},t)$ composed of the external field V_ext, the Hartree potential V_H and an exchange-correlation (xc) potential V_xc. The current is a vector field and, accordingly, TDCDFT complements the Kohn-Sham equations by a vector potential $\mathbf{A}_\mathrm{S}$ to

$$\mathrm{i}\hbar\frac{\partial\varphi_\alpha(\mathbf{r},t)}{\partial t} = \left\{\frac{1}{2m}\left[-\mathrm{i}\hbar\nabla - \frac{q}{c}\mathbf{A}_\mathrm{S}(\mathbf{r},t)\right]^2 + V_\mathrm{S}(\mathbf{r},t)\right\}\varphi_\alpha(\mathbf{r},t)\,, \tag{1a}$$

$$V_\mathrm{S}(\mathbf{r},t) = V_\mathrm{ext}(\mathbf{r},t) + V_\mathrm{H}(\mathbf{r},t) + V_\mathrm{xc}(\mathbf{r},t)\,, \tag{1b}$$

$$\mathbf{A}_\mathrm{S}(\mathbf{r},t) = \mathbf{A}_\mathrm{ext}(\mathbf{r},t) + \mathbf{A}_\mathrm{xc}(\mathbf{r},t)\,, \tag{1c}$$

where $q=-e$ is the electron charge and c the light velocity. The vector potential $\mathbf{A}_\mathrm{S}$ is composed of an external contribution $\mathbf{A}_\mathrm{ext}$ and the exchange-correlation vector potential $\mathbf{A}_\mathrm{xc}$. In the following we will use the Vignale-Kohn (VK) approximation for the xc potentials.[4]

The density and the current density can be expressed in terms of the Kohn-Sham wave functions as

$$\rho(\mathbf{r},t) = \sum_\alpha |\varphi_\alpha(\mathbf{r},t)|^2 \tag{2a}$$

$$\mathbf{j}(\mathbf{r},t) = \frac{\hbar}{m}\sum_\alpha \mathrm{Im}\left[\varphi_\alpha^*(\mathbf{r},t)\nabla\varphi_\alpha(\mathbf{r},t)\right] - \frac{q}{mc}\,\mathbf{A}_\mathrm{S}(\mathbf{r},t)\,\rho(\mathbf{r},t)\,, \tag{2b}$$

and are independent of the gauge chosen to represent the electromagnetic potentials.

A. The Vignale-Kohn functional in real time

Up to second order in spatial derivatives, under the basic assumption that the gradients of the density and the velocity are small (see Ref. 12), and choosing a gauge with $V_\mathrm{xc}=0$, the VK functional in real time reads

$$\frac{q}{c}\frac{\partial A_{\mathrm{xc},i}(\mathbf{r},t)}{\partial t} = \partial_i V_\mathrm{xc}^\mathrm{ALDA} - \frac{\sum_j \partial_j \sigma_{\mathrm{xc},ij}(\mathbf{r},t)}{\rho(\mathbf{r},t)}\,, \tag{3}$$

where the second term on the right-hand side is usually referred to as the "memory term". It is determined by the visco-elastic xc stress tensor whose components are

$$\sigma_{\mathrm{xc},ij}(\mathbf{r},t) = \int_{-\infty}^{t}\mathrm{d}t'\left\{\eta(\mathbf{r},t,t')\left[\partial_i v_j(\mathbf{r},t') + \partial_j v_i(\mathbf{r},t') - \frac{2}{d}\nabla\cdot\mathbf{v}(\mathbf{r},t')\delta_{ij}\right] + \zeta(\mathbf{r},t,t')\nabla\cdot\mathbf{v}(\mathbf{r},t')\delta_{ij}\right\} \tag{4}$$

where d is the number of spatial dimensions.[13] Here $\mathbf{v}(\mathbf{r},t) = \mathbf{j}(\mathbf{r},t)/\rho(\mathbf{r},t)$ is the time-dependent velocity field. The time-dependent visco-elastic coefficients are the Fourier transforms of the complex visco-elastic coefficients:

$$\eta(\mathbf{r},t,t') = \int\frac{\mathrm{d}\omega}{2\pi}\eta_\mathrm{xc}(\bar\rho,\omega)\mathrm{e}^{-\mathrm{i}\omega(t-t')}\Big|_{\bar\rho=\rho(\mathbf{r},t_*)} \tag{5a}$$

$$\zeta(\mathbf{r},t,t') = \int\frac{\mathrm{d}\omega}{2\pi}\zeta_\mathrm{xc}(\bar\rho,\omega)\mathrm{e}^{-\mathrm{i}\omega(t-t')}\Big|_{\bar\rho=\rho(\mathbf{r},t_*)} \tag{5b}$$

where η stands for the shear viscosity and ζ for the bulk viscosity coefficient (still possibly including elasticity effects). There remains an open question on the choice of the time instant t_*. It may be either $t_*=t$ or $t_*=t'$ or anything in between. The differences involve higher gradient corrections,[12] which are disregarded in the present approach and which become obsolete anyway in the instantaneous approximation which we will use (Sec. II B). The visco-elastic coefficients are expressed in the frequency domain as

$$\eta_\mathrm{xc}(\rho,\omega) = -\frac{\rho^2}{\mathrm{i}\omega}f_\mathrm{xc}^\mathrm{T}(\rho,\omega) \tag{6a}$$

$$\zeta_\mathrm{xc}(\rho,\omega) = -\frac{\rho^2}{\mathrm{i}\omega}\left[f_\mathrm{xc}^\mathrm{L}(\rho,\omega) - \frac{2(d-1)}{d}f_\mathrm{xc}^\mathrm{T}(\rho,\omega) - \frac{\mathrm{d}^2\epsilon_\mathrm{xc}(\rho)}{\mathrm{d}\rho^2}\right]. \tag{6b}$$

Here $\epsilon_\mathrm{xc}(\rho)$ is the xc energy density and $f_\mathrm{xc}^{\mathrm{L},\mathrm{T}}(\rho,\omega)$ are the frequency-dependent longitudinal (L) and transverse (T) response kernels of the homogeneous electron gas evaluated at the density ρ. The xc kernels are not known accurately. There are two works in which practicable approximations are given.[14,15] In the following, we will use the more recent parametrization given by Qian and Vignale (QV),[15] which was designed to satisfy all known limits and relations of the longitudinal and transverse xc kernels, and which allows a simple analytic evaluation of $\eta(\mathbf{r},t,t')$.

B. An instantaneous approximation to the VK functional

With its third order derivatives and double integrals over time, the VK approximation makes the Kohn-Sham equations highly involved. Our goal here is to simplify

the original equations to make their computation feasible while keeping the important aspects of the VK approximation. We are looking for an approximation to $\sigma_{\mathrm{xc},ij}(\mathbf{r},t)$ which is local in time (i.e. instantaneous) as

$$\sigma_{\mathrm{xc},ij}(\mathbf{r},t) \approx \eta_0(\mathbf{r},t)\Big[\partial_i v_j(\mathbf{r},t) + \partial_j v_i(\mathbf{r},t) - \frac{2}{d}\nabla\cdot\mathbf{v}(\mathbf{r},t)\delta_{ij}\Big] + \zeta_0(\mathbf{r},t)\,\nabla\cdot\mathbf{v}(\mathbf{r},t)\delta_{ij}\ . \tag{7}$$

This can be obtained by considering the time-dependent visco-elastic coefficients $\eta(\mathbf{r},t,t')$ and $\zeta(\mathbf{r},t,t')$ in Eq. (4) as significantly different from zero only during a time interval $t' \in [t-T,t]$, with t' so short with respect to the plasma period that the velocity gradients during that time interval can be considered constant. This leads to the identifications

$$\eta_0(\mathbf{r},t) = \int_{-\infty}^{t} \mathrm{d}t'\,\eta(\mathbf{r},t,t') \tag{8a}$$

$$\zeta_0(\mathbf{r},t) = \int_{-\infty}^{t} \mathrm{d}t'\,\zeta(\mathbf{r},t,t')\ . \tag{8b}$$

Using the QV parametrization for $\eta_{\mathrm{xc}}(\rho,\omega)$ and $\zeta_{\mathrm{xc}}(\rho,\omega)$, we can evaluate (8a) and (8b), which read

$$\eta_0(\mathbf{r},t) = \rho(\mathbf{r},t)\ a_3^{\mathrm{T}}\big|_{\rho(\mathbf{r},t)} \tag{9a}$$

$$\zeta_0(\mathbf{r},t) = 0, \tag{9b}$$

where the coefficient a_3^{T} is given in Ref. 15. Note that to arrive at (9a) we assume $\lim_{\omega\to 0}\eta_{\mathrm{xc}}(\rho,\omega) = 0$. This is compatible with the instantaneous approximation (7). Under this approximation, indeed, the visco-elastic coefficients $\eta(\mathbf{r},t,t')$ and $\zeta(\mathbf{r},t,t')$ are assumed peaked for $t-t' \to 0^+$ and to approach zero very quickly. This implies that most of the memory comes from the recent past. This approximation to the static limit of η_{xc} coincides with the QVA/QV0 approximation used in previous works.[7,16,17] Note also that the approximation (9a) corresponds to a transverse kernel $f_{\mathrm{xc}}^{\mathrm{T}}(\rho,\omega) = -\mathrm{i}\omega\eta_{\mathrm{xc}}(\mathbf{r},\omega)/\rho^2$ that is purely imaginary. This feature will be important for the interpretation of the results in Sec. IV, since it is precisely the imaginary part of the complex $f_{\mathrm{xc}}^{\mathrm{L,T}}$ kernels that is responsible for the dissipative effects.[9]

III. IMPLEMENTATION

We have implemented the VK functional in our open-source package TELEMAN.[18] Wave functions and fields are represented on an equidistant Cartesian grid in 3D coordinate space. The operators of momentum and kinetic energy are evaluated in Fourier space exploiting the fast Fourier transformation. For the (scalar) energy-density functional, we use the Perdew-Wang parametrization.[19] The ionic cores are described by separable pseudopotentials of Goedecker type.[20] The static solution is evaluated using accelerated gradient iteration[21] and in order to deal with the numerical $\mathbf{A}_{\mathrm{xc}}$ each time step of the dynamical evolution is done by a fourth order series expansion of the exponential of the Kohn-Sham Hamiltonian. For more technical details see Ref. 22.

Even in its simplified form the implementation of the VK functional in a real-time propagation of finite systems remains demanding, because it involves third order derivatives of the wave functions and because the velocity $\mathbf{v} = \mathbf{j}/\rho$ becomes an unsafe quantity in the tails of the electron cloud where ρ becomes very low. The problems raised by TDCDFT can be understood by looking at Fig. 1, which shows the density and velocity profiles along the symmetry axis of a Na_2 dimer :

1. The velocity is well behaved in the center of the box where density is large, but it is plagued by strong fluctuations and huge values near the edges. This simply comes from the fact that, while both the density and the current basically vanish at the box boundaries, thus physically corresponding to a region of space virtually void of particles, their ratio may take large values. This feature is also present in TDDFT, but it has no practical consequence as the velocity has no impact on the Kohn-Sham field. However, in TDCDFT, the strange velocity profile at the outer tail, amplified by high-order derivatives, leads in a few time steps to insurmountable numerical instabilities.

2. A better understanding of the velocity behavior is

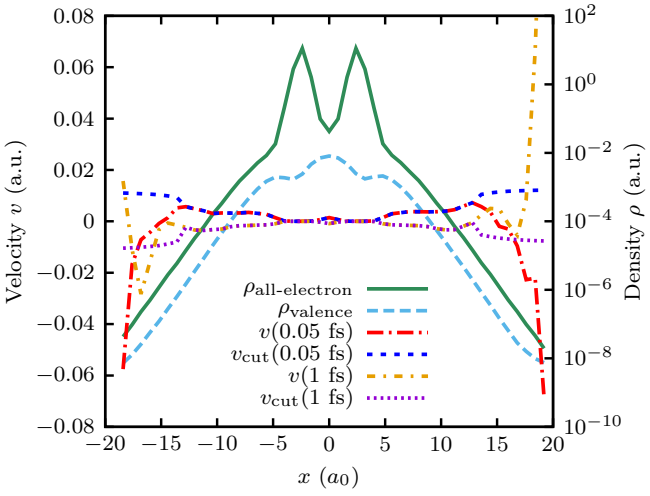

Figure 1. Velocities (at times $t = 0.05$ fs and $t = 1$ fs, left vertical scale) and densities (at $t = 0$, right vertical scale) of Na_2 along its symmetry axis. The molecule is computed in a box 48^3 points with grid spacing of 0.8 a_0. Dynamics is initialized by an instantaneous dipole boost momentum $p_{\mathrm{boost}} = 0.01\ \hbar/a_0$.

attained by looking at the density, which is crossing 10 orders of magnitude on this example. It is becoming extremely small towards the edges of the box and, since the velocity $\mathbf{v}$ involves ρ^{-1}, this makes $\mathbf{v}$ a numerically critical, perhaps even unphysical, object in the outer tail of a finite system.

3. TDDFT calculations are performed on a reduced set of valence electrons while the remaining core electrons are modeled through a pseudo-potential. The concept of a density thus becomes ambiguous: It could mean the total density ρ of all electrons or the (smaller) density of valence electrons only ρ_{val}. The problem is in fact rather fundamental as pseudo-potentials are usually not tuned to any quantity involving currents. Their use in a TDCDFT environment has thus to be "adapted" to this new context. After a careful analysis of this difficulty in actual computations, we finally decided to follow a split-minded strategy. We compute the (conventional) scalar Kohn-Sham potential using the valence density ρ_{val} (as usually done when using pseudo-potentials) and use the total density ρ in all above outlined expressions of the current functional (as naturally stems from TDCDFT equations). Note also that a pseudopotential description is valid for moderate ionisation regimes, and therefore the use of high intensity fields introduces further difficulties.[23,24]

Therefore, although the implementation of the TDCDFT equations is in principle straightforward, one has to carefully handle the points raised above to avoid that the equations violently diverge in less than one time step of propagation. We have obtained a stable code by using two essential measures : (i) for the derivatives in the current functionals, we use second-order finite differences derivatives, which, in presence of fluctuations, are more robust than the high order Fourier definition ; (ii) in the computation of the velocity, we employ a numerical smoothing technique to eliminate the spurious signal in the low density area, which progressively puts the velocity to a constant while ensuring its continuity along all axes.

IV. RESULTS

We tested our implementation by calculating the time evolution of the dipole moment for three closed-shell systems, namely the Ca atom, the Mg atom, and the Na_2 dimer. We excite the systems by an instantaneous initial boost of the valence electron cloud and then let the system evolve freely. This avoids interference with an external photon field and thus allows us to check the stability of the code as such, and the physics it describes. Moreover, from the dipole moment, we can extract excitation energies and compare them with previous works which use the VK functional in linear response. The numerical parameters are optimized for each system. We use 64^3 grid points for Ca and Mg but 48^3 for Na_2. The grid spacing is 0.6 a_0, 0.5 a_0, and 0.8 a_0 for Ca, Mg, and Na_2, respectively. All three systems deal with two active valence electrons and use a time step of 0.02 $\hbar$/Ry. The boost strength is varied and will be specified in each case separately.

A. Damping of the dipole moment

Figure 2 shows the time evolution of the dipole moment of Ca, calculated using TDDFT within ALDA and TDCDFT within the VK approximation.

Ca is distinguished by having one very dominant dipole mode with only very little spectral fragmentation. This avoids damping of the dipole signal by distribution over many sub-modes (Landau damping[25,26]) and makes it the ideal test case for checking dissipative contributions from TDCDFT. And indeed, the dipole signal from mere TDDFT carries on to oscillate without visible damping. In TDCDFT, we however observe a strong damping of the dipole moment. This was already observed in previous works on model systems,[8,10] although it had been shown to be overestimated in small systems while becoming correct in the thermodynamic limit.[10] The VK approximation, hence, can describe dissipation even in a real-time description and in the instantaneous approximation (7). We also see that the position of the oscillation peaks remains the same as in TDDFT. This can be understood from the fact that the approximation (9a)-(9b) to the visco-elastic coefficient η_0 and ζ_0 corresponds to a purely imaginary transverse kernel $f_{\mathrm{xc}}^{\mathrm{T}}$, and that only a real part can have an effect on the position of the oscillation peaks.[11]

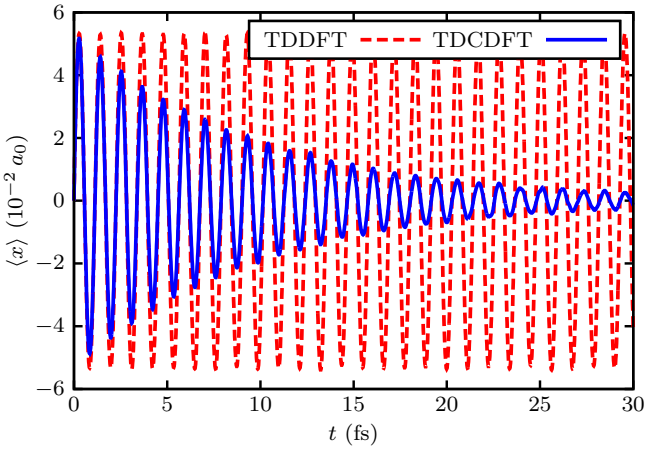

Figure 2. Dipole moment of Ca as a function of time for TDDFT and TDCDFT. Both cases used the (small) initial boost of $p_{\mathrm{boost}} = 0.01\ \hbar/a_0$.

Table I. Excitation energies (eV) for the lowest $s \to p$ transitions of Ca and Mg.

		This work	Previous work[11]	
	Expt.[31]	$\omega_{\rm VK}$	$\omega_{\rm VK}$	$\omega_{\rm ALDA}$
Ca	2.933	3.66−0.068i	2.962−0.063i	3.381
Mg	4.346	4.45−0.047i	4.509−0.093i	4.571

B. Linear response

From the dipole signal after a faint instantaneous boost one can compute the spectral distribution of dipole strength by Fourier transformation of the dipole signal. This is the real-time approach to linear response spectra.[27–29] We have done that for the case of Ca and Mg atoms. In Ca, there is a clear dominant dipole transition such that it suffices to look just at position and width of this prominent dipole peak. In Mg, the situation is more involved as, besides a strong $3s \to 3p$ transition, there exist several nearby transitions ($3s \to 4p, 5p, 6p$) which are only about one order of magnitude less intense than the main one (we have checked that these transitions match tabulated transitions in Mg[30]). Our initial boost excites all dipole modes simultaneously. Thus the various transitions contribute with comparable weights and it will be difficult to single out the effect of a single, dominant mode.

The results for Ca and Mg are compiled in Table I with those for TDDFT in the column $\omega_{\rm ALDA}$ and for TDCDFT in the columns $\omega_{\rm VK}$. We also compare our results with the work of Ullrich *et al.*,[11] where the full VK functional has been implemented within linear response, and with experimental measurements.[31] It is worth noting that in Ref. 11, the authors explore well identified transitions while our boost analysis excites a mix of modes. TDDFT has purely real frequencies while the TDCDFT results acquire an imaginary part. Thus the effect of the VK approach with respect to ALDA is to broaden the peaks. The position of the peaks remains almost the same as in ALDA for our instantaneous approach. There is a small shift of the real part for the case of Ca in Ref. 11, whereas the imaginary parts (widths) are comparable in both calculations in the case of Ca. As for Mg, the damping in our computations is larger than that of the individual $3s \to 3p$ transition of Ref. 11, an effect which can be attributed to our simultaneous account of the dominant transition and nearby ones. These results confirm the findings from Fig. 2 from the frequency perspective. Our implementation of TDCDFT thus seem to be robust since two different calculations give similar results.

C. Non-linear effects

An important physical issue and a strong motivation of the present investigation concerns the possible access to dissipative behaviors in non linear dynamical scenarios. Therefore, we have explored this aspect by increasing the value of the initial boost. Note that in this work, we do not use absorbing boundary conditions. The system we explore is thus closed and we can focus on how initial excitation energy does redistribute towards "thermal" degrees of freedom, without being polluted by the competing de-excitation channel provided by direct electron emission.

Figure 3 compares the evolution of the dipole moment in TDCDFT for various initial boost strengths and in two test cases, that is the Mg atom and the Na_2 dimer.

Note that the dipole moments are rescaled proportionally to the inverse of the initial boost. They would thus become identical for an undamped motion. We see only little dependence on the initial boost. This is plausible when looking at the model for the viscosities as given in Eq. (6) together with the approximation (9) because there is no entry for the actual excitation energy visi-

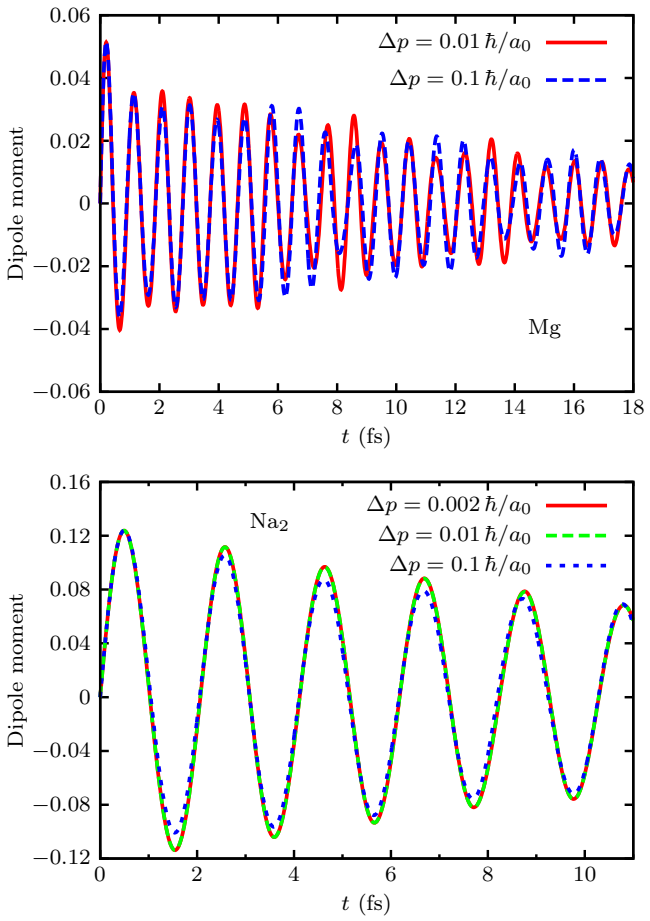

Figure 3. Time evolution of dipole moments calculated in TDCDFT after instantaneous boost for Mg (upper panel) and Na_2 (lower panel). Different boost strengths are compared, as indicated in the respective panels. The dipole moments are scaled by boost strength to become comparable.

ble. But this is unphysical, since theories with a detailed microscopic description of electron-electron collisions, namely for Fermi liquids in bulk[32] and for finite electron systems,[33–35] show that damping depends sensitively on excitation status because the phase space for collisions opens up with increasing energy (or temperature). The instantaneous VK approximation to TDCDFT does not reproduce this expected trend. Thus it is limited to the linear regime and should better not be used for non-linear excitations. This is consistent with the way in which the VK functional has been derived, i.e. for a weakly perturbed electron gas.

D. Total energy

We finally looked at the time evolution of the total energy. Figure 4 shows the adiabatic total energy as defined in Refs. 8, 10, and 36.

As expected, the total energy remains constant with TDDFT in ALDA, whereas using VK, the initial total energy (the contribution to the kinetic energy due to the initial boost) is dissipated in the course of time. D'Agosta and Vignale[36] proved that the adiabatic Kohn-Sham energy decreases monotonically in the absence of an external field when the VK approach is used, which indicates that the system is irreversibly driven to equilibrium. This scenario has already been observed in previous TDCDFT works on one-dimensional models,[8,10] where it is argued that the energy loss is distributed over configuration space (thermalization), however, without accounting for compensation by thermalization of the system.

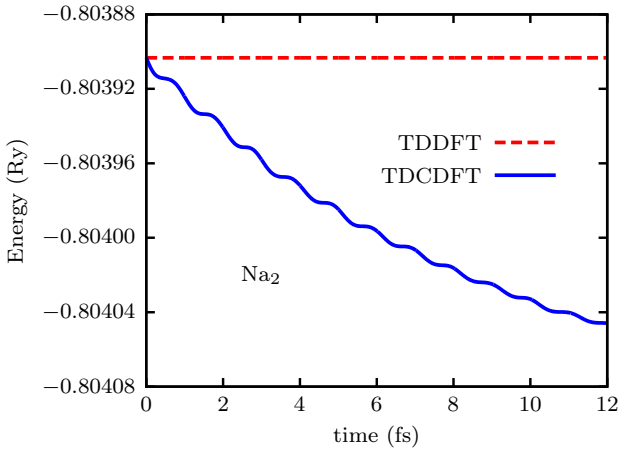

Figure 4. Time evolution of the total energy as a function of time for TDDFT and TDCDFT in the Na_2 dimer initially excited with a boost of $p_{\mathrm{boost}} = 0.01\ \hbar/a_0$.

V. CONCLUSIONS

We have implemented TDCDFT in real time and three spatial dimensions. We have used the approximation to the exchange-correlation vector potential proposed by Vignale and Kohn which takes into account non-adiabatic effects. Due to the numerical challenges that such an implementation represents, we have developed a new approximation for the non-adiabatic term that, while treating the memory instantaneously in time, maintains the dissipating effects of the VK approximation. We have demonstrated the capabilities of the method by applying it to Mg, Ca and Na_2 whereby we are modeling a short laser pulse by an instantaneous boost. Within the linear regime (small boosts), our results compare well with previous results obtained using the VK functional within linear response theory. This indicates that our implementation as well as our approximation to the VK functional are robust. However, in the non-linear regime the VK approximation is found to fail.. Indeed, it is expected that damping should significantly depend on the amount of deposited excitation energy in a system: the larger the excitation energy, the faster the relaxation. This general feature is not reproduced within our implementation of TDCDFT. Better approximations to the exchange-correlation functional need to be devised. However one has to consider also the increasing complexity of the equations to deal with from a numerical point of view, which may cause this route to dissipation unpractical. This has yet to be explored. The quest for a reliable and manageable theoretical framework to describe quantum dissipation in finite systems remains a challenge.

ACKNOWLEDGEMENTS

We thank French research funding agency ANR and Institut Universitaire de France for support during the realization of this work. J.M.E. acknowledges the support of EPSRC Grant EP/J015059/1. P.R. and J.M.E. would like to thank J.A. Berger for fruitful discussions.

REFERENCES

[1] H. Haken and H.C. Wolf, *The Physics of Atoms and Quanta* (Springer, Berlin, 2000).
[2] F. Krausz and M. Ivanov, Rev. Mod. Phys. **81**, 163 (2009).
[3] G. Vignale, Phys. Lett. A **209**, 206 (1995).
[4] G. Vignale and W. Kohn, Phys. Rev. Lett. **77**, 2037 (1996).
[5] M. van Faassen, P. L. de Boeij, R. van Leeuwen, J.A. Berger, and J. G. Snijders, Phys. Rev. Lett. **88**, 186401 (2002).
[6] M. van Faassen, P. L. de Boeij, R. van Leeuwen, J.A. Berger, and J. G. Snijders, J. Chem. Phys. **118**, 1044 (2003).
[7] J.A. Berger, P. Romaniello, R. van Leeuwen, and P. L. de Boeij, Phys. Rev. B **74**, 245117 (2006).
[8] H. O. Wijewardane and C. A. Ullrich, Phys. Rev. Lett. **95**, 086401 (2005).
[9] C.A. Ullrich and I.V. Tokatly, Phys. Rev. B **73**, 235102 (2006).
[10] C. A. Ullrich, J. Chem. Phys. **125**, 234108 (2006).

[11]C.A. Ullrich, and K. Burke, J. Chem. Phys. **121**, 28 (2004)
[12]G. Vignale, C. A. Ullrich, and S. Conti, Phys. Rev. Lett. **79**, 4878 (1997).
[13]G.F. Giuliani and G. Vignale, *Quantum Theory of the Electron Liquid* (Cambridge University Press, 2005).
[14]S. Conti, R. Nifosì, M.P. Tosi, J. Phys: Cond. Matt. **9**, L475 (1997).
[15]Z. Qian and G. Vignale, Phys. Rev. B **65**, 235121 (2002); *ibid.* **71**, 169904(E) (2005).
[16]J.A. Berger, P. L. de Boeij, and R. van Leeuwen, Phys. Rev. B **71**,155104 (2005).
[17]J.A. Berger, P. L. de Boeij, and R. van Leeuwen, Phys. Rev. B **75**, 035116 (2007).
[18]See http://www.pw-teleman.org for the code and a detailed description thereof.
[19]J.P. Perdew, Y. Wang, Phys. Rev. B **45**, 13244 (1992).
[20]S. Goedecker, M. Teter, J. Hutter, Phys. Rev. B **54**, 1703 (1996).
[21]V. Blum, G. Lauritsch, J. A. Maruhn, P.-G. Reinhard, J. Comp. Phys **100**, 364 (1992).
[22]F. Calvayrac, P.-G. Reinhard, E. Suraud, C.A. Ullrich, Phys. Rep. **337**, 493 (2000).
[23]E. Fowe Penka, E. Couture-Bienvenue, and A D. Bandrauk, Phys. Rev. A **89**, 023414 (2014).
[24]T. Zuo, A.D. Bandrauk, and P.B. Corkum, Chem. Phys. Lett. **259**, 313 (1996).
[25]P.G. Reinhard and E. Suraud, *Introduction to Cluster Dynamics*, (Wiley, New York, 2004).
[26]V.O. Nesterenko, W. Kleinig, and P.-G. Reinhard, Eur. Phys. J. D **19**, 57 (2002).
[27]F. Calvayrac, P.-G. Reinhard, E. Suraud, Phys. Rev. B **52**, R17056 (1995).
[28]K. Yabana, G. F. Bertsch, Phys. Rev. B **54**, 4484 (1996).
[29]F. Calvayrac, P.-G. Reinhard, E. Suraud, Ann. Phys. (NY) **255**, 125 (1997).
[30]See the NIST Atomic Spectra Database, available at http://www.nist.gov/pml/data/asd.cfm.
[31]C. E. Moore, *Natl. Stand. Ref. Data Ser., Natl. Bur. Stand. (U.S.) 35* (National Bureau of Standards, 1971), Vol. I–III; S. Bashkin and J. D. Stoner, *Atomic Energy Levels and Grotrian Diagrams* (North-Holland, Amsterdam, 1975).
[32]D. Pines and P. Nozières, *The Theory of Quantum Liquids* (W.A. Benjamin, New York, 1966).
[33]A. Domps, P.-G. Reinhard, and E. Suraud, Phys. Rev. Lett. **81**, 5524 (1998).
[34]T. Fennel, G. F. Bertsch, and K.-H. Meiwes-Broer, Eur. Phys. J. D **29**, 367 (2004).
[35]P.-G. Reinhard and E. Suraud, Ann. Phys. (N. Y.) **354**, 183 (2015).
[36]R. D'Agosta and G. Vignale, Phys. Rev. Lett. **96**, 016405 (2006).